View metadata, citation and similar papers at core.ac.uk
brought to you by CORE

東北大学機関リポジトリ
TOUR
Tohoku University Repository

Effect of heavy boron doping on pressure-induced phase transitions in single-crystal silicon

著者	宇田　聡
journal or publication title	Applied physics letters
volume	87
number	19
page range	191911-1-191911-3
year	2005
URL	http://hdl.handle.net/10097/47032

doi: 10.1063/1.2120920

Effect of heavy boron doping on pressure-induced phase transitions in single-crystal silicon

X. Q. Yan, X. M. Huang, S. Uda, and M. W. Chen[a]
Institute for Materials Research, Tohoku University, Sendai 980-8577, Japan

(Received 9 June 2005; accepted 6 September 2005; published online 3 November 2005)

The influence of applied loads and loading/unloading rates on pressure-induced phase transitions in lightly and heavily boron-doped silicon was systematically investigated. The resultant phases were plotted into two-dimensional maps with applied loads and loading/unloading rates as the coordinate axes. The formation region of the amorphous phase in the heavily boron-doped silicon was found to be much larger than that in the lightly boron-doped one, suggesting that heavy boron doping promotes the amorphization in silicon. © *2005 American Institute of Physics*.
[DOI: 10.1063/1.2120920]

It is well known that cubic silicon (Si-I) subjected to high pressures experiences a series of crystal structure changes. Diamond-anvil cell studies have suggested that Si-I can transform into a metallic β-Sn phase (Si-II) at elevated pressures.[1–4] During pressure release Si-II further transforms into several metastable phases including amorphous silicon (a-Si), body-centered-cubic Si-III phase, rhombohedral distortion Si-XII phase,[5] and hexagonal diamond phase Si-IV.[6] Moreover, these pressure-induced phase transitions can also be achieved by indentation testing.[7–9] The combination of depth-sensing indentation testing and Raman spectroscopy has been successfully employed to study pressure-induced phase transitions in Si,[10–16] which provides a simple and effective way to investigate the complicated phase transitions. Extensive investigations have established that these transformations during pressure release strongly depend on unloading rates.[10–16] The a-silicon phase appears with rapid unloading whereas a mixture of Si-III and Si-XII with slow unloading. However, to the best knowledge of the authors, all the results on pressure-induced phase transitions in Si were obtained from lightly doped silicon or standard Si wafers. The effect of heavy boron doping on the phase transitions has not been explored before.

Currently, heavily boron-doped silicon has been used as substrates for $p/p+$ epitaxial wafers of large-scale integrated circuit devices, and employed as etch stop in the fabrication of silicon microengineered devices.[17] It has been reported that heavy boron doping can effectively suppress dislocation activity in silicon,[18] which allows the heavily boron-doped silicon to withstand large stresses prior to dislocation generation and thus to be able to serve as seed crystals for growing dislocation-free Si single crystals without using thin necks.[19] Because these applications require mechanical performance, efforts to characterize mechanical properties of heavily boron-doped silicon and its damage mechanisms under mechanical loading are gradually being realized. In this study, we systematically investigated the influence of applied loads and loading/unloading rates of nanoindentation tests on the phase transitions in lightly and heavily boron-doped silicon wafers combining with Raman spectroscope analysis.

[a]Author to whom correspondence should be addressed; electronic mail: mwchen@imr.tohoku.ac.jp

Two kinds of single-crystal (111) silicon wafers with light boron doping (1×10^{15} atoms/cm^3) and heavy boron doping (9×10^{18} atoms/cm^3) were used in our experiments. They were ultrasonically cleaned for 20 min in acetone, then dipped into 5% HF for 30 min to remove the oxide layers, and followed by a thorough rinse in de-ionized water. Nanoindentation tests were performed using a dynamic ultramicro hardness tester (DUH-W201S, Shimadzu) equipped with a Berkovich diamond indenter (face angle 65.03°). A constant load-rate mode was chosen for the tests. The maximum applied loads range from 20 to 100 mN and the loading/unloading rates from 0.13 to 13.24 mN/s. To determine the critical phase transformation pressures, load-displacement data were processed to obtain the curves of average contact pressure versus contact depth.[20] The residual impressions produced at different load levels with various loading/unloading rates were examined by a micro-Raman spectrometer (Renishaw, UK) with an Ar$^+$ laser (excitation wavelength 514.5 nm). The size of the laser spot is about 1 μm, smaller than the dimension of impressions ($1\sim4$ μm). In the Raman experiments, a low laser power of 2 mW was used to avoid any possible artifacts caused by laser heating, and all Raman spectra were acquired from the center of the residual impressions as determined by optical microscopy.

For lightly boron-doped Si, three types of load-displacement curves were obtained, corresponding to different phase transitions as suggested by Domnich *et al.*[12] Figure 1(a) shows typical examples tested at 60 mN with loading/unloading rates at 0.66, 3.31, and 6.62 mN/s. At a low loading/unloading rate of 0.66 mN/s, a pop-out phenomenon, sudden displacement discontinuity, was observed in the unloading part. This has been attributed to the formation of Si-III and Si-XII from Si-II.[12] At a fast loading/unloading rate of 6.62 mN/s, an elbow (the gradual change in the slope of unloading curve) occurred, revealing the appearance of a-Si. At the medium rate of 3.31 mN/s, the mixed feature of pop out and elbow can be seen, suggesting the formation of the mixture of Si-III, Si-XII, and a-Si. These phase transitions were confirmed by the postmortem Raman characterization, which will be discussed later. The critical pressures corresponding to the three types of phase transitions, Si-II $\rightarrow$ Si-III + Si-XII, Si-II $\rightarrow$ Si-III + Si-XII + a-Si, and

 © 2005 American Institute of Physics
Downloaded 17 Feb 2010 to 130.34.135.83. Redistribution subject to AIP license or copyright; see http://apl.aip.org/apl/copyright.jsp

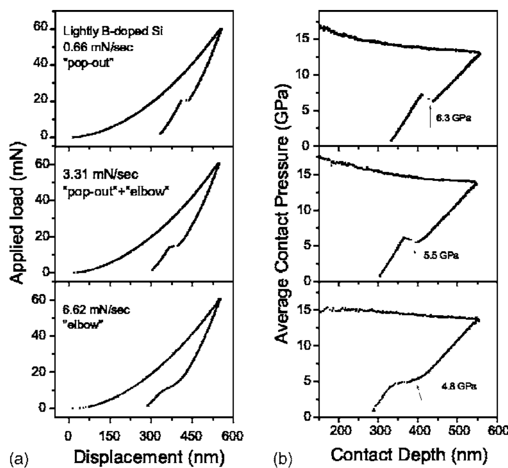

FIG. 1. (a) Nanoindentation load-displacement curves of the lightly boron-doped Si with various loading/unloading rates and (b) corresponding average contact pressure vs contact depth curves at the load level of 60 mN.

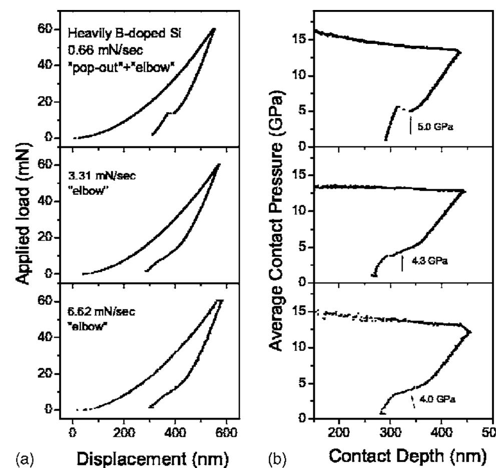

FIG. 3. (a) Load-displacement curves of the heavily boron-doped Si with various loading/unloading rates and (b) corresponding average contact pressure vs contact depth curves at the applied load of 60 mN.

Si-II → *a*-Si, were determined to be about 6.3, 5.5, and 4.8 GPa, respectively, as shown in Fig. 1(b).

Typical examples of Raman spectra from lightly boron-doped Si are shown in Fig. 2. When indentation experiments were performed to the same load (e.g., 60 mN), the resultant silicon phases gradually change with the loading/unloading rates [see Fig. 2(a)]. As the rates decrease below 0.66 mN/s, only metastable crystalline phases Si-XII and Si-III can be observed. The bands at 165, 182, 354, 375, 397, 435, and 485 cm^{-1} have been assigned to Si-XII, and the bands at 165, 382, and 435 cm^{-1} to Si-III. These two phases have very similar structures and some Raman lines represent the overlapping vibrational modes.[13] When the rates vary in the range from 1.32 to 3.31 mN/s, additional broadening peaks at 160, 300, and 470 cm^{-1} appear, corresponding to the amorphous silicon.[21] Thus three phases (*a*-Si, Si-XII and Si-III) coexist at medium loading/unloading rates. When the rates being further increased to above 3.31 mN/s, Si-XII and Si-III completely disappear and only amorphous silicon can be identified. At constant loading/unloading rates, the resultant silicon phases gradually change with loading levels. Figure 2(b) shows an example tested at 3.31 mN/s. With decreasing load levels, the peaks of Si-XII and Si-III phases diminish slowly and the amorphous Si peaks become stronger. As the load level decreases below 40 mN, only the *a*-Si can be observed and Si-XII and Si-III completely disappear. In addition to the peaks that have been assigned to *a*-Si, Si-XII, and Si-III, in these spectra the peak at 520 cm^{-1} is believed from the Si-I matrix, and the peak around 490 cm^{-1} may come from *a*-Si or nano-Si-I phase as suggested by Ref. 15.

For the heavily boron-doped Si, a new type of phase transition has not been found through systematical nanoindentation tests and Raman characterization. Only three types of transitions, the same as the lightly boron-doped Si, were observed with changing load levels and loading/unloading rates. However, the phase formation conditions were measured to be different from the lightly doped one as shown in Fig. 3. At the load level of 60 mN and the loading/unloading rate of 0.66 mN/s, the typical pop-out phenomenon appearing in the lightly doped Si cannot be found. Instead, the load-displacement curve shows the mixed feature of pop out and elbow, corresponding to the formation of the mixture of Si-III, Si-XII, and *a*-Si. At the loading/unloading rates of 3.31 and 6.62 mN/s, only the elbow feature, indicating the formation of sole *a*-Si, appears in the load-displacement curves.

The resultant phases characterized by Raman spectroscopy (Fig. 4) are consistent with these features of the load-displacement curves. At the load of 60 mN, with loading/unloading rates increasing, the peak intensities of the crystalline phases gradually decrease and the amorphous peaks become stronger as shown in Fig. 4(a). It can be observed that *a*-Si can be formed at a much lower loading/unloading rate (0.26 mN/s) in the heavily boron-doped silicon than that (3.31 mN/s) in the lightly boron-doped one. The difference in the phase formation conditions can also be

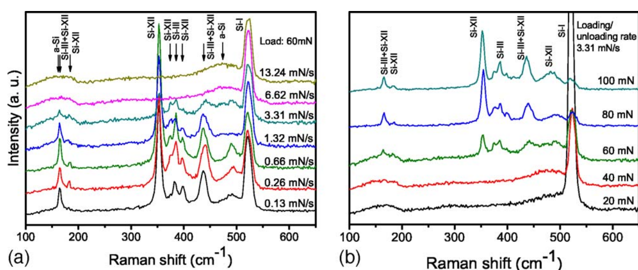

FIG. 2. Raman spectra taken from the residual imprints in the lightly boron-doped Si. (a) At the applied load of 60 mN with various loading/unloading rates and (b) at the loading/unloading rate of 3.31 mN/s with various applied loads.

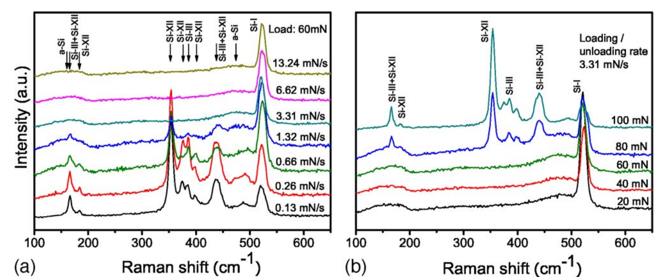

FIG. 4. Raman spectra from the residual impressions in heavily boron-doped Si. (a) At the load level of 60 mN with various loading/unloading rates and (b) at the loading/unloading rate of 3.31 mN/s with various applied loads.

Downloaded 17 Feb 2010 to 130.34.135.83. Redistribution subject to AIP license or copyright; see http://apl.aip.org/apl/copyright.jsp

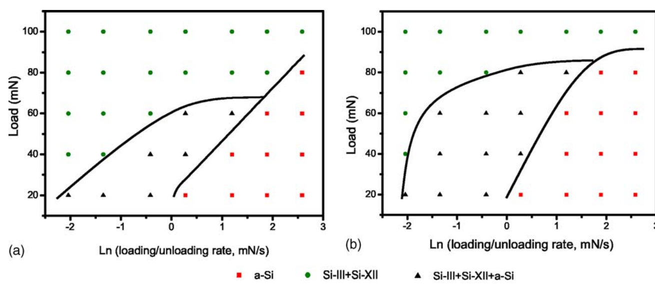

FIG. 5. The maps of pressure-induced phase transitions in silicon as the functions of applied loads and loading/unloading rates. (a) Lightly boron-doped Si and (b) heavily boron-doped Si.

identified from the experiments with a fixed loading/unloading rate and variable loading levels. Figure 4(b) shows an example tested at the loading/unloading rate of 3.31 mN/s. At the load of 60 mN, the amorphous Si is the sole product of the pressure-induced phase transitions, while in the lightly doped one the transition products are the mixed Si-III, Si-XII, and *a*-Si at this load level [Fig. 2(b)]. Thus, the amorphization appears to be much easier in the heavily boron-doped Si than lightly boron-doped one, and amorphous Si can be generated at relatively lower loading/unloading rates and higher load levels.

To illustrate the phase-transition difference in the two samples, the resultant phases identified by Raman characterization and nanoindentation tests were plotted into two-dimensional maps with applied loads and loading/unloading rates as the coordinate axes, as shown in Fig. 5. From the phase-transition maps, it can be clearly observed that the *a*-Si related transitions have much larger formation regions in the heavily doped Si than in the lightly doped Si. Evidently, boron doping promotes the amorphization of silicon. Additionally, the corresponding critical pressures for the three types of phase transitions, Si-II $\rightarrow$ Si-III+Si-XII, Si-II $\rightarrow$ Si-III+Si-XII+*a*-Si, and Si-II $\rightarrow$ *a*-Si, were measured to be about 6.2, 5.0, and 4.2 GPa. The pressures (5.0 and 4.2 GPa) associated with the *a*-Si formation are much lower than those (5.5 and 4.8 GPa) of the lightly doped one, which may be intrinsically related to the easy formation of *a*-Si.

The effect of boron doping on the promoted amorphization of Si appears to be associated with two facts: large atomic size difference (25%) between boron (0.88 Å) and silicon (1.17 Å), and softening of shear elastic constants caused by boron doping. It is known that the basic principle of pressure-induced amorphization is to increase the free energy of a crystalline phase to a point higher than that of an amorphous phase.[22–24] The large atomic size mismatch and thereby elastic strains around the substitutional boron atoms will certainly increase the free energy and thermodynamically encourage the amorphization. Additionally, the localized strains will reduce the elastic stability of the Si crystal structure in the vicinity of B atoms, resulting in the nucleation of pressure-induced *a*-Si at the substitutional sites and kinetically put forward the amorphization of Si. Furthermore, the softening of shear elastic constants caused by boron-doping may also be important for the easy amorphization in the heavily boron-doped Si. It is well known that elastic properties of Si depend on the free-electron or hole concentration.[24,25] Boron doping can lead to the concentration change of carriers in Si, and results in the reduction of the elastic properties that has been evidenced by Raman measurements.[25,26] The amorphization of Si may be assisted by the softening of shear elastic constants, which, coupling with the large elastic strains, leads to the violation of the Born stability conditions,[27,28] and results in crystal collapse.

In summary, the phase-transition maps with the applied loads and loading/unloading rates as the functions were developed to quantitatively describe the phase transitions in nanoindented Si with light and heavy boron dopings. It was found that boron doping significantly promotes the formation of *a*-Si. Although the underlying mechanism has not been fully understood, based on the current knowledge on the pressured-induced solid-state amorphization, the large atomic size difference between boron and silicon and the reduction of the shear elastic constant causing by boron doping appear to play important roles in the enhanced amorphization.

[1]J. C. Jamieson, Science **139**, 762 (1963).
[2]J. Z. Hu, L. D. Merkle, C. S. Menoni, and I. L. Spain, Phys. Rev. B **34**, 4679 (1986).
[3]H. Olijnyk, S. K. Sikka, and W. B. Holzaffel, Phys. Lett. **103A**, 137 (1984).
[4]J. Z. Hu and I. L. Spain, Solid State Commun. **51**, 263 (1984).
[5]J. Grain, G. J. Ackland, J. R. Maclean, R. O. Piltz, P. D. Hatton, and D. S. Pawley, Phys. Rev. B **50**, 13043 (1994).
[6]G. Weill, J. L. Mansot, G. Sagon, C. Carlone, and J. M. Besson, Semicond. Sci. Technol. **4**, 280 (1989).
[7]I. V. Gridneva, Y. V. Milman, and V. I. Trefilov, Phys. Status Solidi A **14**, 177 (1972).
[8]A. P. Gerk and D. Tabor, Nature (London) **271**, 732 (1978).
[9]M. C. Gupta and A. L. Ruoff, J. Appl. Phys. **51**, 1072 (1980).
[10]A. Kailer, Y. Gogotsi, and K. Nickel, J. Appl. Phys. **81**, 3057 (1997).
[11]Y. Gogotsi, V. Domnich, S. Dub, A. Kailer, and K. Nickel, J. Mater. Res. **15**, 871 (2000).
[12]V. Domnich, Y. Gogotsi, and S. Dub, Appl. Phys. Lett. **76**, 2214 (2000).
[13]V. Domnich and Y. Gogotsi, Rev. Adv. Mater. Sci. **3**, 1 (2002).
[14]A. B. Mann, D. Van Heerden, J. B. Pethica, P. Bowes, and T. P. Weihs, Philos. Mag. A **82**, 1921 (2002).
[15]J. Jang, M. J. Lance, S. Q. Wen, T. Y. Tsui, and G. M. Pharr, Acta Mater. **53**, 1759 (2005).
[16]T. Juliano, V. Domnich, and Y. Gogotsi, J. Mater. Res. **19**, 3099 (2004).
[17]M. A. Lourenco, D. J. Gardiner, V. Gouvernayre, and M. Bowden, J. Mater. Sci. Lett. **19**, 771 (2000).
[18]I. Yonenaga, T. Taishi, X. Huang, and K. Hoshikawa, J. Appl. Phys. **89**, 5788 (2001).
[19]K. Hoshikawa, X. Huang, T. Taishi, T. Kajigaya, and T. Iino, Jpn. J. Appl. Phys., Part 2 **38**, L1369 (1999).
[20]W. C. Oliver and G. M. Pharr, J. Mater. Res. **7**, 1564 (1992).
[21]M. Hanfland and K. Syassen, High Press. Res. **3**, 242 (1990).
[22]C. Massobrio, V. Pontikis, and G. Martin, Phys. Rev. Lett. **62**, 1142 (1989).
[23]J. Koike, Phys. Rev. B **47**, 7700 (1993).
[24]R. W. Keyes, in *Solid State Physics*, edited by F. Seitz and D. Turnbull (Academic, New York, 1967), Vol. 20, p. 37.
[25]F. Cerdeira and M. Cardona, Phys. Rev. B **5**, 1440 (1972).
[26]X. Huang, K. Wu, M. Chen, T. Toshinori, K. Hoshikawa, S. Koh, and S. Uda, Mater. Sci. Semicond. Process. (to be published).
[27]J. Wang, S. Yip, S. R. Phillpot, and D. Wolf, Phys. Rev. Lett. **71**, 4182 (1993).
[28]J. S. Tse and D. D. Klug, Phys. Rev. Lett. **67**, 3559 (1991).

Downloaded 17 Feb 2010 to 130.34.135.83. Redistribution subject to AIP license or copyright; see http://apl.aip.org/apl/copyright.jsp